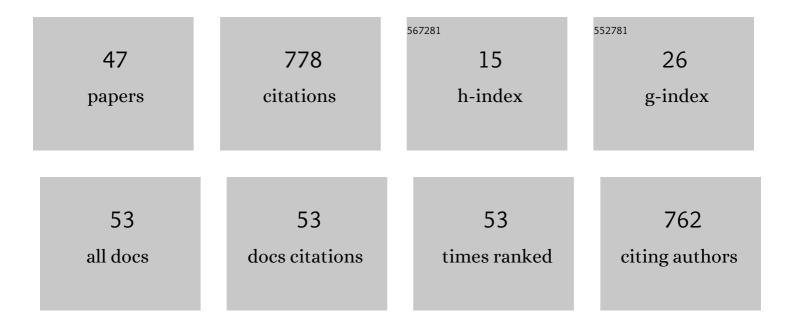
Takefumi Yoshida

List of Publications by Year in descending order

Source: https://exaly.com/author-pdf/8846700/publications.pdf

Version: 2024-02-01



#	Article	IF	CITATIONS
1	Electro-Oxidation Reaction of Methanol over La _{2–<i>x</i>} Sr _{<i>x</i>} NiO _{4+δ} Ruddlesden–Popper Oxides. ACS Applied Energy Materials, 2022, 5, 503-515.	5.1	15
2	Elucidating 2D Chargeâ€Densityâ€Wave Atomic Structure in an MX–Chain by the 3Dâ€Î"Pair Distribution Function Method**. ChemPhysChem, 2022, 23, .	2.1	6
3	Heterospin frustration in a metal-fullerene-bonded semiconductive antiferromagnet. Nature Communications, 2022, 13, 495.	12.8	5
4	Insight into the Gd–Pt Bond: Slow Magnetic Relaxation of a Heterometallic Gd–Pt Complex. Bulletin of the Chemical Society of Japan, 2022, 95, 513-521.	3.2	3
5	161Dy synchrotron-radiation-based Mössbauer absorption spectroscopy. Hyperfine Interactions, 2022, 243, 1.	0.5	2
6	Macro- and atomic-scale observations of a one-dimensional heterojunction in a nickel and palladium nanowire complex. Nature Communications, 2022, 13, 1188.	12.8	15
7	Elucidating 2D Chargeâ€Đensityâ€Wave Atomic Structure in an MX–Chain by the 3Dâ€Î"Pair Distribution Function Method. ChemPhysChem, 2022, 23, e202200120.	2.1	0
8	Hidden Heterometallic Interaction Emerging from Resonant Inelastic X-ray Scattering in Luminescent Tb–Pt Molecules. Journal of Physical Chemistry C, 2022, 126, 7973-7979.	3.1	0
9	Ni(III) Mott–Hubbard-like State Containing High-Spin Ni(II) in a Semiconductive Bromide-Bridged Ni-Chain Compound. Inorganic Chemistry, 2022, 61, 9504-9513.	4.0	8
10	An unusual Pd(<scp>iii</scp>) oxidation state in the Pd–Cl chain complex with high thermal stability and electrical conductivity. Dalton Transactions, 2021, 50, 1614-1619.	3.3	9
11	Emergence of Metallic Conduction and Cobalt(II)-Based Single-Molecule Magnetism in the Same Temperature Range. Journal of the American Chemical Society, 2021, 143, 4891-4895.	13.7	21
12	One-Step Synthesis of a Three-Dimensionally Hyperbranched Fe(II)-Based Metallo-Supramolecular Polymer Using an Asymmetrical Ditopic Ligand for Durable Electrochromic Films with Wide Absorption, Large Optical Contrast, and High Coloration Efficiency. ACS Applied Electronic Materials, 2021, 3, 2044-2055.	4.3	13
13	Ru(II)-Based Metallo-Supramolecular Polymer with Tetrakis(<i>N</i> -methylbenzimidazolyl)bipyridine for a Durable, Nonvolatile, and Electrochromic Device Driven at 0.6 V. ACS Applied Materials & Interfaces, 2021, 13, 31153-31162.	8.0	16
14	Precise Synthesis of Alternate Fe(II)/Os(II)â€Based Bimetallic Metalloâ€ 5 upramolecular Polymer. Macromolecular Rapid Communications, 2020, 41, 1900384.	3.9	15
15	Proton Conductivity of Metallo-Supramolecular Polymer Boosted by Lithium Ions. ACS Applied Polymer Materials, 2020, 2, 326-334.	4.4	14
16	An Organic–Inorganic Hybrid Exhibiting Electrical Conduction and Singleâ€ion Magnetism. Angewandte Chemie, 2020, 132, 2420-2427.	2.0	5
17	An Organic–Inorganic Hybrid Exhibiting Electrical Conduction and Singleâ€Ion Magnetism. Angewandte Chemie - International Edition, 2020, 59, 2399-2406.	13.8	19
18	Electrochromic Os-based metallo-supramolecular polymers: electronic state tracking by <i>in situ</i> XAFS, IR, and impedance spectroscopies. RSC Advances, 2020, 10, 24691-24696.	3.6	6

Takefumi Yoshida

#	Article	IF	CITATIONS
19	One-Pot Synthesis of Three-Dimensionally Hyperbranched Eu/Fe-Based Heterometallo-Supramolecular Polymers as Thermally Tough Proton-Conducting Nanoparticles. ACS Applied Polymer Materials, 2020, 2, 4439-4448.	4.4	5
20	Simultaneous manifestation of metallic conductivity and single-molecule magnetism in a layered molecule-based compound. Chemical Science, 2020, 11, 11154-11161.	7.4	13
21	Dual-Redox System of Metallo-Supramolecular Polymers for Visible-to-Near-IR Modulable Electrochromism and Durable Device Fabrication. ACS Applied Materials & Interfaces, 2020, 12, 58277-58286.	8.0	29
22	Conductive zigzag Pd(iii)–Br chain complex realized by a multiple-hydrogen-bond approach. CrystEngComm, 2020, 22, 3999-4004.	2.6	10
23	Dual-Branched Dense Hexagonal Fe(II)-Based Coordination Nanosheets with Red-to-Colorless Electrochromism and Durable Device Fabrication. ACS Applied Materials & Interfaces, 2020, 12, 31896-31903.	8.0	36
24	Ni(II)-Based Metallosupramolecular Polymer with Carboxylic Acid Groups: A Stable Platform for Smooth Imidazole Loading and the Anhydrous Proton Channel Formation. ACS Omega, 2020, 5, 14796-14804.	3.5	5
25	Transparent Supercapacitor Display with Redox-Active Metallo-Supramolecular Polymer Films. ACS Applied Materials & Interfaces, 2020, 12, 16342-16349.	8.0	41
26	Reversible four-color electrochromism triggered by the electrochemical multi-step redox of Cr-based metallo-supramolecular polymers. RSC Advances, 2020, 10, 10904-10909.	3.6	6
27	Emergence of electrical conductivity in a flexible coordination polymer by using chemical reduction. Chemical Communications, 2020, 56, 8619-8622.	4.1	19
28	Periodicity of Singleâ€Molecule Magnet Behaviour of Heterotetranuclear Lanthanide Complexes across the Lanthanide Series: A Compendium. Chemistry - A European Journal, 2020, 26, 6036-6049.	3.3	9
29	Ionic-caged heterometallic bismuth–platinum complex exhibiting electrocatalytic CO ₂ reduction. Dalton Transactions, 2020, 49, 2652-2660.	3.3	9
30	Electrochromic devices using Fe(II)â€based metalloâ€supramolecular polymer: Introduction of ionic liquid as electrolyte to enhance the thermal stability. Journal of the Society for Information Display, 2019, 27, 661-666.	2.1	14
31	Thermally stable electrochromic devices using Fe(II)-based metallo-supramolecular polymer. Solar Energy Materials and Solar Cells, 2019, 200, 110000.	6.2	34
32	Observation of charge bistability in quasi-one-dimensional halogen-bridged palladium complexes by X-ray absorption spectroscopy. Dalton Transactions, 2019, 48, 11628-11631.	3.3	5
33	Porous Molecular Conductor: Electrochemical Fabrication of Through-Space Conduction Pathways among Linear Coordination Polymers. Journal of the American Chemical Society, 2019, 141, 6802-6806.	13.7	94
34	Construction of Coordination Nanosheets Based on Tris(2,2′-bipyridine)–Iron (Fe ²⁺) Complexes as Potential Electrochromic Materials. ACS Applied Materials & Interfaces, 2019, 11, 11893-11903.	8.0	61
35	Synchrotron-radiation-based Mössbauer absorption spectroscopy with high resonant energy nuclides. Hyperfine Interactions, 2019, 240, 1.	0.5	2
36	Ln–Pt electron polarization effects on the magnetic relaxation of heterometallic Ho– and Er–Pt complexes. Dalton Transactions, 2019, 48, 7144-7149.	3.3	10

Takefumi Yoshida

#	Article	IF	CITATIONS
37	Slow Magnetic Relaxation in a Palladium–Gadolinium Complex Induced by Electron Density Donation from the Palladium Ion. Chemistry - A European Journal, 2018, 24, 9285-9294.	3.3	34
38	Modulation of a coordination structure in a europium(<scp>iii</scp>)-based metallo-supramolecular polymer for high proton conduction. RSC Advances, 2018, 8, 37193-37199.	3.6	16
39	Slow magnetic relaxation in a Tb(<scp>iii</scp>)-based coordination polymer. Dalton Transactions, 2018, 47, 16066-16071.	3.3	2
40	Diversity in Design of Electrochromic Devices with Metallo-Supramolecular Polymer: Multi-Patterned and Tube-Shaped Displays. Journal of Photopolymer Science and Technology = [Fotoporima Konwakai Shi], 2018, 31, 343-347.	0.3	5
41	Slow Magnetic Relaxation in a Palladium–Gadolinium Complex Induced by Electron Density Donation from the Palladium Ion. Chemistry - A European Journal, 2018, 24, 9169-9169.	3.3	Ο
42	Fieldâ€induced Slow Magnetic Relaxation of Gd ^{III} Complex with a Ptâ^'Gd Heterometallic Bond. Chemistry - A European Journal, 2017, 23, 4551-4556.	3.3	32
43	Multiple Magnetic Relaxation Pathways and Dualâ€Emission Modulated by a Heterometallic Tbâ€Pt Bonding Environment. Chemistry - A European Journal, 2017, 23, 10527-10531.	3.3	15
44	Temperature dependence of Peierls–Hubbard phase transition in [Pd(cptn)2Br]Br2studied by scanning tunneling microscopy. Japanese Journal of Applied Physics, 2016, 55, 08NB16.	1.5	6
45	Optically Visible Phase Separation between Mott-Hubbard and Charge-Density-Wave Domains in a Pd-Br Chain Complex. ChemistrySelect, 2016, 1, 259-263.	1.5	18
46	Direct Observation of Ordered Highâ€Spin–Lowâ€Spin Intermediate States of an Iron(III) Threeâ€Step Spinâ€Crossover Complex. Angewandte Chemie, 2016, 128, 5270-5275.	2.0	17
47	Direct Observation of Ordered Highâ€Spin–Lowâ€Spin Intermediate States of an Iron(III) Threeâ€Step Spinâ€Crossover Complex. Angewandte Chemie - International Edition, 2016, 55, 5184-5189.	13.8	59